1306 *J. Med. Chem.* **2010,** *53,* 1306–1318
DOI: 10.1021/jm9015729

Journal of
Medicinal
Chemistry
Article

Synthesis and Antitumor Activity of a Novel Series of 6-Substituted Pyrrolo[2,3-*d*]pyrimidine Thienoyl Antifolate Inhibitors of Purine Biosynthesis with Selectivity for High Affinity Folate Receptors and the Proton-Coupled Folate Transporter over the Reduced Folate Carrier for Cellular Entry

Lei Wang,[†,¶] Christina Cherian,[∥,¶] Sita Kugel Desmoulin,[‡] Lisa Polin,[∥,⊥] Yijun Deng,[‡] Jianmei Wu,[∥] Zhanjun Hou,[∥] Kathryn White,[∥,⊥] Juiwanna Kushner,[∥,⊥] Larry H. Matherly,*[,‡,§,∥,▽] and Aleem Gangjee*[,†,▽]

[†]*Division of Medicinal Chemistry, Graduate School of Pharmaceutical Sciences, Duquesne University, 600 Forbes Avenue, Pittsburgh, Pennsylvania 15282,* [∥]*Developmental Therapeutics Program, Barbara Ann Karmanos Cancer Institute, 110 East Warren Ave, Detroit, MI 48201,* [‡]*Graduate Program in Cancer Biology, Wayne State University School of Medicine, Detroit, Michigan 48201,* [§]*Department of Pharmacology, Wayne State University School of Medicine, Detroit, Michigan 48201, and* [⊥]*Department of Internal Medicine, Division of Hematology-Oncology, Wayne State University School of Medicine, Detroit, Michigan 48201.* [¶]*These authors contributed equally to this work.* [▽]*These authors contributed equally to this work.*

Received October 23, 2009

2-Amino-4-oxo-6-substituted pyrrolo[2,3-*d*]pyrimidines with a thienoyl side chain and four to six carbon bridge lengths (compounds **1**−**3**) were synthesized as substrates for folate receptors (FRs) and the proton-coupled folate transporter (PCFT). Conversion of acetylene carboxylic acids to α-bromomethylketones and condensation with 2,4-diamino-6-hydroxypyrimidine afforded the 6-substituted pyrrolo[2,3-*d*]pyrimidines. Sonogashira coupling with (*S*)-2-[(5-bromo-thiophene-2-carbonyl)-amino]-pentanedioic acid diethyl ester, followed by hydrogenation and saponification, afforded **1**−**3**. Compounds **1** and **2** potently inhibited KB and IGROV1 human tumor cells that express FRα, reduced folate carrier (RFC), and PCFT. The analogs were selective for FR and PCFT over RFC. Glycinamide ribonucleotide formyltransferase was the principal cellular target. In SCID mice with KB tumors, **1** was highly active against both early (3.5 log kill, 1/5 cures) and advanced (3.7 log kill, 4/5 complete remissions) stage tumors. Our results demonstrate potent *in vitro* and *in vivo* antitumor activity for **1** due to selective transport by FRs and PCFT over RFC.

Introduction

Antifolates, typified by methotrexate (MTX),[a] pemetrexed (PMX), and raltitrexed (RTX) (Figure 2) remain important components of the chemotherapeutic arsenal for cancer. MTX continues to be used in therapy of pediatric acute lymphoblastic leukemia, osteogenic sarcoma, and breast cancer.[1] PMX is used for pleural malignant mesothelioma in the US.[2] In addition, PMX is active toward chemotherapy-naïve paients with advanced-stage non-small-cell lung cancer[3] and for maintenance therapy of non-small-cell lung cancer.[4] RTX is an important agent for chemotherapy of advanced colorectal cancer outside of the US.[5]

Since classical antifolates are all anions at physiologic pH, their ability to cross cell membranes by passive diffusion is limited, so specific transporters are required for their activity. There are three major uptake systems for reduced folates, all of which are shared by antifolates.[6−8] The reduced folate carrier or RFC is the major transport system for folates in mammalian cells and tissues at physiologic pH.[6−8] Folate receptors (FRs) α and *β* are glycosylphosphatidylinositol-anchored proteins that transport folates by receptor-mediated endocytosis.[9,10] Finally, the proton-coupled folate transporter or PCFT (SLC46A1) functions optimally at acidic pH.[11,12]

*To whom correspondence should be addressed. L.H.M., phone 313-578-4280, fax 313-578-4287, e-mail matherly@kci.wayne.edu. A.G., phone 412-396-6070, fax 412-396-5593, e-mail gangjee@duq.edu.

RFC is expressed ubiquitiously in tissues and tumors,[7] however, folate uptake by FRs shows a more restricted tissue distribution.[9,10] For instance, FRα is expressed in normal apical membranes of the kidney, choroid plexus, and placenta, whereas FR*β* is expressed in placenta, spleen, and thymus.[10] FR*β* in normal hematopoietic cells cannot bind folate ligand.[13] FRα is expressed in solid tumors such as nonmucinous adenocarcinomas of the ovary, uterus, and cervix, whereas FR*β* is expressed in leukemia blasts in chronic myelogenous leukemia and in acute myelogenous leukemia.[10] Although PCFT is expressed in many normal tissues including liver, kidney, and placenta, PCFT is most abundant in the duodenum and upper jejunum, where it serves as the primary means of intestinal uptake of dietary folates at the acid pH characterizing the upper small intestine.[8] The tumor distribution of human PCFT (hPCFT) has not been systematically studied, however, a prominent low-pH transport component for folates, most likely PCFT, was described in 29 of 32 human solid tumor cell lines.[12]

In recent years, there has been an increased focus on identification of new molecular targets and development of tumor-selective small molecule inhibitors for cancer. Both FRs and PCFT can be used for tumor targeting. For instance, FRs have been targeted with folate-conjugated cytotoxins, liposomes, and radionuclides.[14−16] While cytotoxic antifolates can also be transported by FRs, most folate-based therapeutics are also substrates for the ubiquitously expressed

 Published on Web 01/19/2010

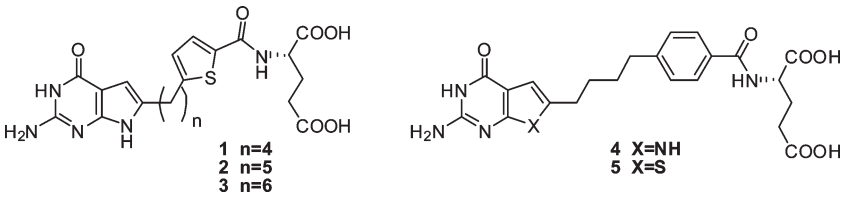

Figure 1. Structures of novel 6-substituted pyrrolo[2,3-*d*]pyrimidines with a thienoyl ring in the side chain, **1**, **2**, and **3**, and previously reported[17,18] benzoyl ring analogs **4** and **5**.

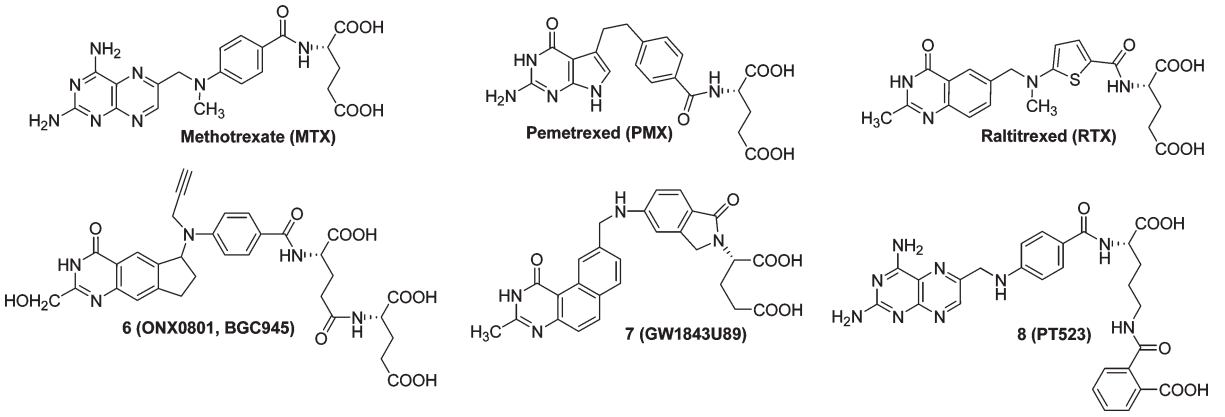

Figure 2. Structures of classical antifolates.

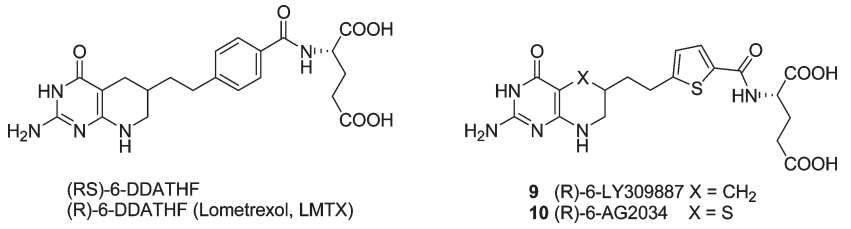

Figure 3. GARFTase Inhibitors.

RFC such that tumor selectivity is lost.[17−19] Nonetheless, there have been unambiguous examples of FR-selectivity including the thymidylate synthase (TS) inhibitors N^{10}-propargyl-5,8-dideazafolic acid (CB3717)[20,21] and **6** {ONX0801 (BGC945)},[22,23] neither of which are effective substrates for RFC. When **6** was tested in mice, there was no systemic toxicity.[23] Although antitumor activity could not be determined (due to high circulating thymidine), [^{125}I]iodo-5′-deoxyuridine incorporation into KB tumor was significantly and selectively increased, establishing inhibition of TS.[23] Whereas RFC-targeted agents have been described without PCFT transport activity {**7**, (GW1843U89), **8**, (PT523)} (Figure 2),[12,18] outside of brief meeting reports[24,25] (see below), no analogous PCFT-specific cytotoxic antifolates capable of selectively targeting solid tumors characterized by acidic microenvironments (albeit without RFC transport activity) have been reported.

We recently described 6-substituted classical pyrrolo[2,3-*d*]pyrimidine[17] and thieno[2,3-*d*]pyrimidine[18] cytotoxic antifolates with varying lengths of the carbon bridge region (Figure 1 shows only the four-carbon bridge forms **4** and **5**), and characterized by selective transport by FRα and FRβ over RFC. For both series, the three- and four-carbon bridge analogs were most active toward FR-expressing human tumors and cytotoxicity was primarily due to the potent inhibition of glycinamide ribonucleotide formyltransferase (GARFTase), the first folate-dependent reaction in *de novo* purine nucleotide biosynthesis, although for thieno[2,3-*d*]-pyrimidine antifolates, a secondary target, most likely 5-amino-4-imidazolecarboxamide ribonucleotide formyltransferase (AICARFTase), was implied.[17,18] The three-carbon pyrrolo-[2,3-*d*]pyrimidine derivative was subsequently reported to also be a substrate for PCFT, thus providing another means of tumor targeting.[24]

A number of antifolates have been previously described as targeting GARFTase. The first GARFTase inhibitor to enter clinical trials was the 6-(*R*)-isomer of 5,10-dideazatetrahydrofolic acid (DDATHF), termed lometrexol (LMTX)[26] (Figure 3). Toxicity in clinical trials led to the discovery of **9** (LY309887) (Figure 3), an analog in which the 1,4-phenyl ring of LMTX was replaced by a 2,5-thienyl ring. The thienyl ring provided greater potency and decreased toxicity compared with LMTX. Compound **9** was active against a variety of tumor xenograft models and subsequently entered clinical trials.[27] Another GARFTase inhibitor to enter clinical trials after demonstrating activity against a variety of tumor models was **10** (AG2034) (Figure 3), a sulfur isostere of **9** also containing a thienyl side chain ring.[28,29] Though these analogs are all active against FRα expressing tumors, they are also avid substrates for the RFC and thus lack tumor selectivity. Indeed, the lack of clinical success of LMTX, **9**, and **10** has been attributed in major part to the toxicity of these analogs,[26−29] likely due to their transport by RFC in normal tissues. Clearly compounds that target the FRα (and possibly PCFT) and are

Scheme 1[a]

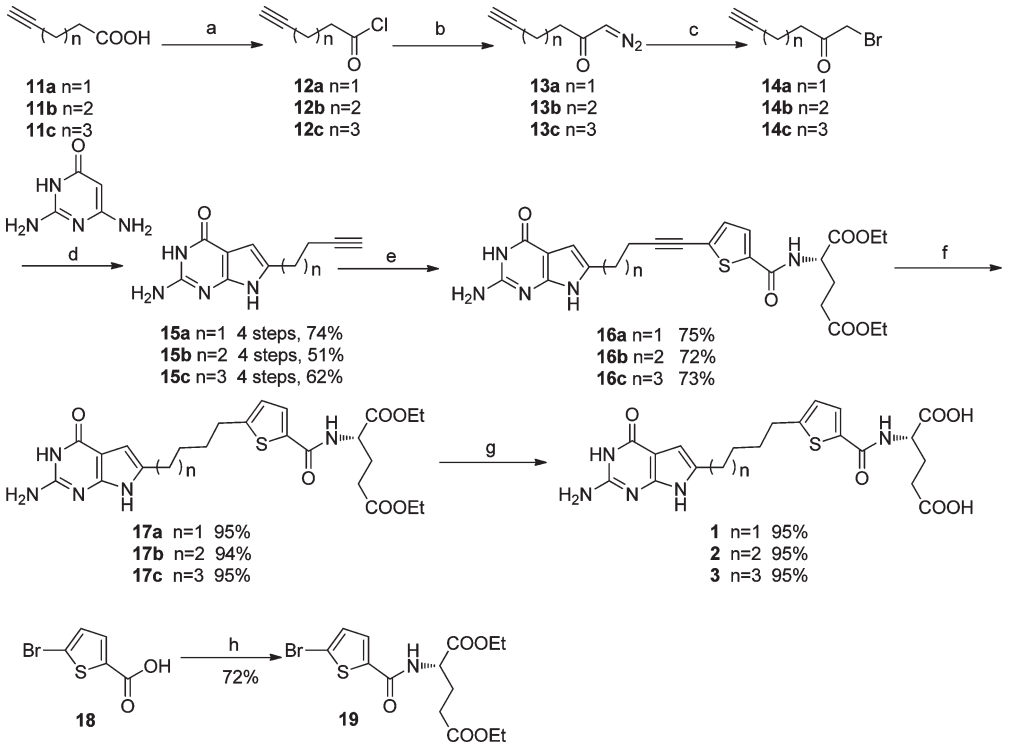

[a] Reagents and conditions: (a) oxalyl chloride, CH_2Cl_2, reflux, 1 h; (b) diazomethane, Et_2O, rt, 1 h; (c) 48% HBr, 80 °C, 2 h; (d) DMF, rt, 3 d; (e) **19**, CuI, $Pd(0)(PPh_3)_4$, Et_3N, DMF, rt, 12 h; (f) 5% Pd/C, H_2, 55 psi, 2 h; (g) (i) 1 N NaOH, rt, 6 h; (ii) 1 N HCl; (h) *N*-methylmorpholine, 2-chloro-4, 6-dimethoxy-1,3,5-triazine, L-glutamate diethyl ester hydrochloride, DMF, rt, 12 h.

not substrates for the RFC have potential to decrease toxicity and afford viable clinically useful antitumor agents.

In this paper, we document our continued drug discovery efforts toward identifying antifolates with poor transport activity by the ubiquitously expressed RFC relative to the other major (anti)folate transport systems with GARFTase as the cytotoxic target. We isosterically replaced the benzoyl ring of previously reported[17] pyrrolo[2,3-*d*]pyrimidines (such as **4**) with a thienoyl ring, in an attempt to improve the GARFTase inhibitory potency while maintaining specificity for FR and PCFT over RFC. We describe the synthesis and biological evaluation of a novel series of 2-amino-4-oxo-6-substituted pyrrolo[2,3-*d*]pyrimidines with bridge length variations from four to six carbons (compounds **1**−**3**; Figure 1). Our biological results establish a remarkable potency of the four-carbon analog **1** of this series as an inhibitor of tumor cell proliferation, resulting from FR- and PCFT-mediated cellular uptake, and inhibition of GARFTase. This compound was devoid of transport via the RFC. Compound **1** is much more potent *in vitro* compared with the most active of the previously published four-atom pyrrolo[2,3-*d*]pyrimidine **4**[17] and the thieno[2,3-*d*]pyrimidine **5**,[18] both of which contain a benzoyl ring in the side chain (Figure 1). Significant *in vivo* antitumor activity was recorded for compound **1** with severe combined immunodeficient (SCID) mice bearing both early and advanced stage KB tumors.

Chemistry

Target compounds **1**−**3** were synthesized as shown in Scheme 1. Commercially available pent-4-ynoic acid **11a** or hex-5-ynoic acid **11b** or hept-6-ynoic acid **11c** (Scheme 1) was converted to the acid chlorides **12a**−**c** and immediately reacted with diazomethane to afford, *in situ*, the α-diazoketones **13a**−**c**, followed by 48% HBr to give the desired α-bromomethylketones **14a**−**c**. Condensation of 2,4-diamino-6-hydroxypyrimidine with **14a**−**c** at room temperature for 3 days afforded the 6-substituted pyrrolo[2,3-*d*]pyrimidines **15a**−**c** (51−74% yield). Compounds **16a**−**c** were obtained by a Sonogashira coupling of **15a**−**c** with (*S*)-2-[(5-bromothiophene-2-carbonyl)-amino]-pentanedioic acid diethyl ester **19**. Hydrogenation and saponification of **16a**−**c** afforded **1**, **2**, and **3**, respectively. Compound **19** (Scheme 1) was synthesized by coupling the commercially available 5-bromo-2-thiophenecarboxylic acid **18** and L-glutamate diethyl ester hydrochloride in 72% yield.

Biological Evaluation and Discussion

Identification of 6-Substituted Pyrrolo[2,3-*d*]pyrimidine Thienoyl Antifolates As Potent Inhibitors of Tumor Cell Proliferation. Three 2-amino-4-oxo-6-substituted pyrrolo-[2,3-*d*]pyrimidines with a thienoyl side chain and bridge length variations from four to six carbons (compounds **1**, **2**, and **3**, respectively) were initially tested as inhibitors of cell growth toward KB and IGROV1 human tumor cells that express FRα, human RFC (hRFC), and hPCFT (unpublished results) using a fluorescence-based cytotoxicity screen. Growth inhibitory effects were compared with those for the classical antifolate inhibitors MTX, LMTX, PMX, RTX, **7**, and **8** (Figures 2 and 3).

In standard culture media for screening FR-targeted agents {folate-free RPMI1640, 10% dialyzed fetal bovine serum, supplemented with 2 nM leucovorin [(6*R*,*S*)5-formyl tetrahydrofolate] (LCV)}, compounds **1** and **2** were active toward both KB (IC_{50}s of 0.55 and 3.2 nM, respectively) and IGROV1 (IC_{50}s of 0.97 and 176 nM, respectively) cells (Table 1). For compound **1**, activity far exceeded that for

Table 1. IC_{50}'s (in nM) for 6-Substituted Pyrrolo[2,3-*d*]pyrimidine Thienoyl Antifolates **1**, **2**, and **3** and Classical Antifolates in hRFC, hPCFT, and FR-Expressing Cell Lines[a]

	Hrfc		hFRα		hFRβ		hPCFT		hRFC/FRα/hPCFT		hRFC/FRα/hPCFT	
antifolate	PC43-10	R2	RT16	RT16 (+FA)	D4	D4 (+FA)	R2/hPCFT4	R2(VC)	KB	KB (+FA)	IGROV1	IGROV1 (+FA)
1	> 1000	> 1000	1.82(0.28)	> 1000	0.57(0.09)	> 1000	43.4(4.1)	> 1000	0.55(0.10)	> 1000	0.97(0.12)	> 1000
2	> 1000	> 1000	4.53(1.60)	> 1000	2.16(0.58)	> 1000	101.4(17.9)	> 1000	3.17(0.32)	> 1000	176(66)	> 1000
3	> 1000	> 1000	137(40)	> 1000	> 1000	> 1000	> 1000	> 1000	231(88)	> 1000	> 1000	> 1000
MTX	12(1.1)	216(8.7)	114(31)	461(62)	106(11)	211(43)	120.5(16.8)	> 1000	6.0(0.6)	20(2.4)	21(3.4)	22(2.1)
PMX	138(13)	894(93)	42(9)	388(68)	60(8)	254(78)	13.2(2.4)	974.0(18.1)	68(12)	327(103)	102(25)	200(18)
RTX	6.3(1.3)	> 1000	15(5)	> 1000	22(10)	746(138)	99.5(11.4)	> 1000	5.9(2.2)	22(5)	12.6(3.3)	20(4.3)
LMTX	12(2.3)	> 1000	12(8)	188(41)	2.6(1.0)	275(101)	38.0(5.3)	> 1000	1.2(0.6)	31(7)	3.1(0.9)	16(6)
7	11(3.3)	> 1000	277(81)	> 1000	52(12)	> 1000	> 1000	> 1000	5.8(3.5)	32(15)	5.2(1.7)	6.9(1.6)
8	1.28(0.18)	> 1000	409(51)	864(39)	[b]	> 1000	> 1000	> 1000	5.26(1.07)	2.90(0.16)	3.47(0.48)	2.47(0.38)

[a] Growth inhibition assays were performed for CHO sublines engineered to express hRFC (PC43-10), FR (RT16, D4), or hPCFT (R2/hPCFT4), for comparison with transporter null [R2, R2(VC)] CHO cells, and for the KB and IGROV1 tumor sublines (expressing hRFC, FRα, and hPCFT), as described in the Experimental Section. For the FR experiments, growth inhibition assays were performed in the presence and the absence of 200 nM folic acid (FA). The data shown are mean values from 2−10 experiments (plus/minus SEM in parentheses). Results are presented as IC_{50} values, corresponding to the concentrations that inhibit growth by 50% relative to cells incubated without drug. Data for MTX, PMX, RTX, LMTX, and **7** were previously published.[17,18] [b] Not determined.

Figure 4. Growth inhibition of KB cells by the 6-substituted pyrrolo[2,3-*d*]pyrimidine thienoyl antifolate **1** in the presence of physiologic concentrations of reduced folate. Cell proliferation inhibition was measured over a range of concentrations of compound **1** in complete folate-free RPMI1640 in the presence of LCV at 2, 25, and 50 nM. Cell densities were measured with CellTiter Blue fluorescence dye and a fluorescence plate reader. Results were normalized to cell density in the absence of drug. Results shown are representative data of experiments performed in duplicate.

all the classical antifolate inhibitors. Activity for compound **3** was substantially decreased. For compounds **1** and **2** (and for KB cells, compound **3**), growth inhibitory effects were completely reversed by cotreatment with excess folic acid (200 nM), establishing FR-targeted activity. However, the effects of the classical antifolates were only partially reversed by folic acid, indicating both FR-mediated and FR-independent drug uptake, as previously described.[17,18] The growth inhibitory effect of compound **1** toward KB cells was only slightly attenuated with increased LCV approximating physiologic concentrations of reduced folates (25 and 50 nM) (IC_{50}s of 4.5 and 10.57 nM, respectively) (Figure 4).

To better assess the contributions of the individual folate transporters to the antiproliferative activities of pyrrolo[2,3-*d*]pyrimidine thienoyl antifolates with KB and IGROV1 cells, growth inhibition was assessed in isogenic Chinese hamster ovary (CHO) sublines engineered to express individually human FRα (RT-16), hRFC (PC43-10), or hPCFT (R2/hPCFT4).[17,18,30] CHO cells expressing only FRβ (D4) were also tested.[17,18] All the CHO sublines were derived from the RFC-, FR-, and PCFT-null MTXRIIOua^{R}2-4 (R2) subline.[30,31] The FR binding levels and endogenous RFC- and PCFT-mediated transport activities for these isogenic cell line models were previously reported.[17,18]

As in our prior studies with the CHO sublines,[17,18,30] routine proliferation assays used 10% dialyzed fetal bovine serum in standard RPMI1640 (PC43-10 cells) or folate-free RPMI1640 supplemented with 3 nM (RT16 and D4 cells) or 25 nM (R2/hPCFT4 cells) LCV. For the PC43-10 and R2/hPCFT4 sublines, results were compared with those for R2 cells or R2 cells transfected with empty vector [designated R2(VC)], whereas those for RT16 and D4 cells were compared with those for a parallel incubation in the presence of an elevated concentration (200 nM) of folic acid. As expected, compounds **1** and **2** showed a high level of FR-targeted activity (IC_{50}s of 1.82 and 4.53 nM, respectively, for FRα-expressing RT16 cells and 0.57 and 2.16 nM, respectively, for FRβ-expressing D4 cells), which was abolished with excess folic acid (Table 1). For hPCFT-expressing R2/hPCFT4 cells, compounds **1** and **2** showed IC_{50}s of 43 and 101 nM, respectively, whereas compound **3** was completely inert. None of these analogs showed any growth inhibition toward R2 or R2(VC) cells or toward hRFC-expressing

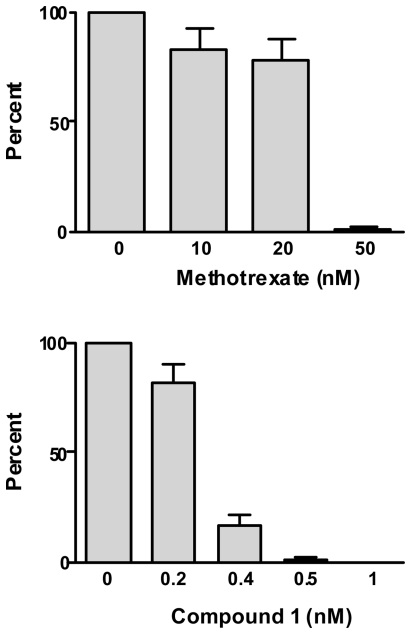

Figure 5. Colony-forming inhibition assay. KB cells were inoculated into 60 mm dishes with a density of 200 cells per dish, in the presence or absence of a range of concentrations of methotrexate (upper panel) or compound **1** (lower panel). Colonies were enumerated after 10−14 days after staining with methylene blue. Data were calculated as percent of controls treated identically but without drugs. Results are presented as mean values from three experiments (plus/minus SEM).

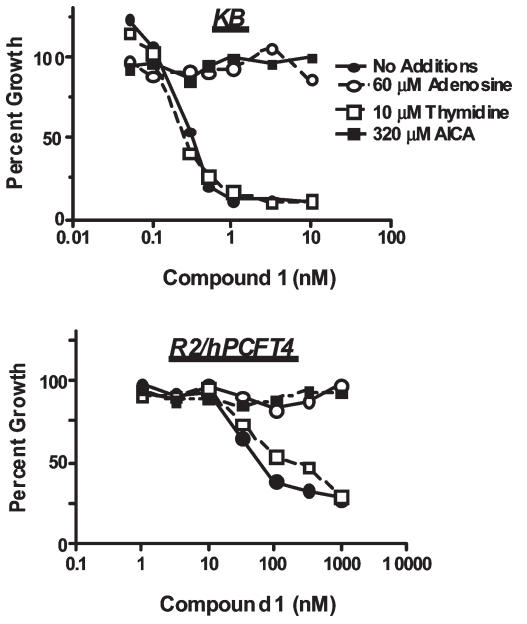

Figure 6. Protection of KB and R2/hRFC4 cells from growth inhibition by the 6-substituted pyrrolo[2,3-*d*]pyrimidine thienoyl antifolate **1** in the presence of nucleosides and 5-amino-4-imidazole (AICA). Proliferation inhibition was measured for KB (upper panel) and R2/hPCFT4 (lower panel) cells over a range of concentrations of compound **1**, as shown, in complete folate-free RPMI1640 with 2 nM (KB) or 25 nM (R2/hPCFT4) leucovorin, in the presence or absence of adenosine (60 μM) or thymidine (10 μM) or AICA (320 nM). Cell densities were measured with CellTiter Blue fluorescence dye and a fluorescence plate reader. Results were normalized to cell density in the absence of drug. Results shown are representative data of experiments performed in triplicate.

PC43-10 cells at concentrations up to 1000 nM. When PC43-10 cells were cultured as for the R2/hPCFT4 cells (e.g., complete folate-free medium with 25 nM LCV as the sole source of folates), there were nominal differences in sensitivities to the 6-substituted pyrrolo[2,3-*d*]pyrimidine thienoyl antifolates (not shown). The results with compounds **1** and **2** are quite different from those for the classical antifolates, MTX, PMX, RTX, LMTX, **7**, and **8**, for which significant yet variable levels of drug activity were detected with FR-expressing RT16 and D4 cells, and with hRFC-expressing PC43-10 cells. For R2/hPCFT4 cells, MTX, PMX, RTX, and LMTX were all active, establishing hPCFT-mediated uptake for these drugs, as previously reported.[18] Of these classical analogs, only PMX showed increased activity toward R2/hPCFT4 cells over that in PC43-10 cells (Table 1). Both **7** and **8** were completely inert toward R2/hPCFT4 cells (Table 1).

Compound **1** was also tested for its capacity to inhibit colony formation of KB cells. Cells were plated at limiting dilutions, and colonies were counted after 10−14 days. Results were compared with those for untreated cells and for KB cells treated with MTX. Colony-forming assays afforded analogous results to those for the cell outgrowth inhibition assays (Table 1). At the highest concentration tested (1 nM), compound **1** gave greater than 99% inhibition of colony formation (Figure 5).

Since nucleoside salvage pathways circumvent the biosynthetic requirements for reduced folates, we tested adenosine and thymidine for their capacities to abolish growth inhibitory effects of the 6-substituted pyrrolo[2,3-*d*]pyrimidine thienoyl antifolates in order to identify the likely targeted (e.g., *de novo* purine or thymidylate) pathway(s). The growth inhibitory effects of compound **1** toward both KB and R2/hPCFT4 cells were completely reversed by the addition of adenosine (60 μM) but not thymidine (10 μM) (Figure 6). This establishes that, following its uptake by FRα or hPCFT, compound **1** derives its antiproliferative effects by inhibiting *de novo* purine nucleotide biosynthesis. For both cell lines, compound **1** was completely protected by 5-amino-4-imidazolecarboxamide (AICA) (320 μM), a metabolite that is metabolized to AICA ribonucleotide (AICAR), an intermediate in the purine biosynthetic pathway and a substrate for the folate-dependent reaction catalyzed by AICAR formyltransferase (AICARFTase), which bypasses the step catalyzed by GARFTase.[17,18] These results identify GARFTase as the likely intracellular enzyme target for **1**. Analogous results were obtained with compound **2** (not shown).

Biochemical Mechanisms. The active compounds **1** and **2** appear to derive their antiproliferative effects via FR- and hPCFT-mediated cellular uptake rather than uptake by hRFC. Antiproliferative effects reflect suppression of *de novo* purine biosynthesis, most likely by inhibition of GARFTase. Additional mechanistic studies were performed to confirm these conclusions.

Competitive inhibition of [^{3}H]folic acid binding to FRs in RT16 (FRα) and D4 (FRβ) cells was used as a direct measure of relative FR binding affinity and by extension endocytotic (anti)folate uptake. For these experiments, cells were washed at pH 3.5 (removes bound folate), then treated with 50 nM [^{3}H]folic acid in the presence of a range of concentrations of unlabeled (anti)folates including compounds **1**−**3**, PMX, MTX, LMTX, and folic acid. Following further washes (neutral pH), bound [^{3}H]folic acid was quantitated (as pmol/mg protein) and relative inhibitor affinities were calculated as the inverse molar ratios of unlabeled ligand

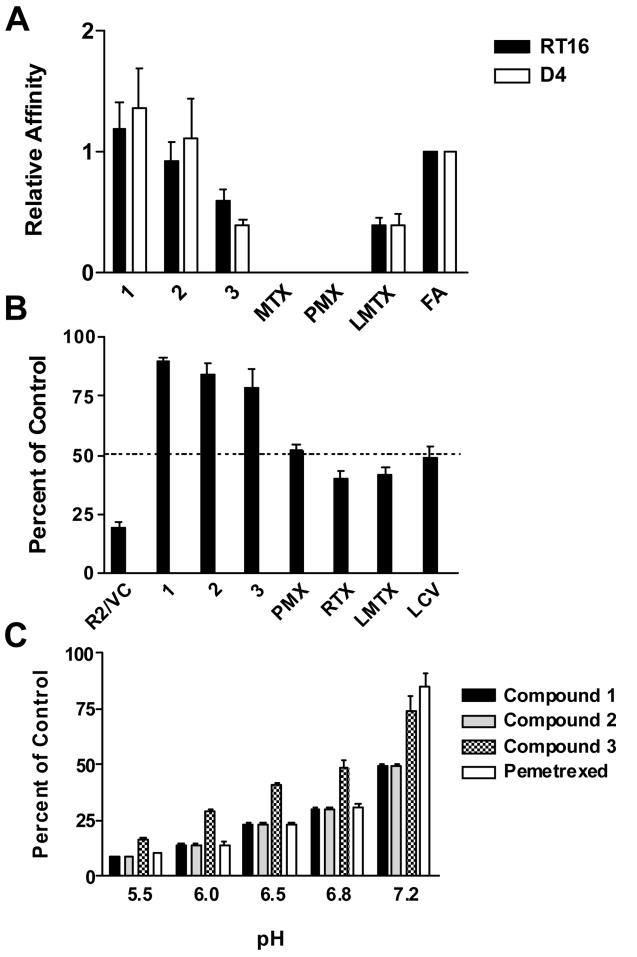

Figure 7. Transport parameters for FR, hRFC, and hPCFT cellular uptake: (A) Data are shown for the effects of the unlabeled ligands with FRα-expressing RT16 CHO cells and FRβ-expressing D4 CHO cells. Relative binding affinities for assorted folate/antifolate substrates were determined over a range of ligand concentrations and were calculated as the inverse molar ratios of unlabeled ligands required to inhibit [^{3}H]folic acid binding by 50%. By definition, the relative affinity of folic acid is 1. (B) PC43-10 cells ectopically expressing hRFC but no FR or PCFT were assayed for [^{3}H]MTX (0.5 μM) uptake at pH 7.2 in the presence of the pyrrolo-[2,3-*d*]pyrimidine antifolates **1**−**3** or the (anti)folates PMX, RTX, LMTX, or LCV (each at 10 μM). (C) R2/hPCFT4 cells ectopically expressing hPCFT but not FR or hRFC were assayed for [^{3}H]MTX (0.5 μM) uptake from pH 5.5 to pH 7.2 in the presence of the pyrrolo[2,3-*d*]pyrimidine thienoyl antifolates **1**−**3** or PMX (each at 10 μM). For panels B and C, results are expressed as a percent of control, incubated in parallel but without addition of inhibitor. Details for the transport and binding assays are provided in the Experimental Section. Results are presented as mean values plus/minus SEM from three experiments.

required to inhibit [^{3}H]folic acid binding by 50%. Despite their differences in cytotoxic activities, compounds **1**−**3** were all potent inhibitors of [^{3}H]folic acid binding with relative affinities [compared with unlabeled folic acid (set to a value of 1)] for FRα of 1.2, 0.9, and 0.6, respectively, and for FRβ of 1.4, 1.1, and 0.4, respectively (Figure 7, panel A). PMX and MTX both showed low affinities for FRα and β, whereas the affinity for LMTX was somewhat higher.

Consistent with results of cell proliferation assays with hRFC-expressing PC43-10 cells, compounds **1**−**3** all were poor competitive inhibitors for [^{3}H]MTX uptake by hRFC at pH 7.2 (Figure 7, panel B). This contrasts with more potent (≥50%) inhibitions by the established hRFC substrates PMX, RTX, LMTX, and LCV.

Table 2. Kinetic Constants for hPCFT[a]

substrate	parameter	pH 5.5	pH 6.8
MTX	K_t (μM)	0.28 ± 0.02	4.52 ± 0.19
MTX	V_{max} (pmol/(mg·min))	31.23 ± 4.31	13.72 ± 2.26
1	K_i (μM)	0.13 ± 0.01	1.95 ± 0.02
2	K_i (μM)	0.10 ± 0.01	2.23 ± 0.20
PMX	K_i (μM)	0.096 ± 0.012	1.54 ± 0.17

[a] Kinetic constants for MTX (K_t and V_{max}) were determined with [^{3}H]MTX by Lineweaver−Burke plots with R2/hPCFT4 cells, whereas K_i values were determined by Dixon plots with [^{3}H]MTX as substrate and a range of inhibitor concentrations in R2/hPCFT4 cells. Results are presented as mean values ± standard errors from three experiments.

Finally, compounds **1**−**3** were compared with PMX as competitive inhibitors of [^{3}H]MTX transport by hPCFT in R2/hPCFT4 cells over a pH range spanning from pH 5.5 to 7.2. Despite marked differences in antiproliferative activities, for all drugs, inhibition of transport was significant and increased dramatically with decreasing pH (Figure 7, panel C). From pH 5.5 to 6.8, the order of inhibition was PMX = **1** = **2** > **3**. Interestingly, the low level of transport activity detected at pH 7.2 (~9% of that at pH 5.5) appeared to be more sensitive to competitive inhibition by compounds **1** and **2** than by either PMX or compound **3**. To calculate K_is for PMX, along with those for compounds **1** and **2**, we measured transport inhibition over a range of inhibitor concentrations at pH 5.5 and pH 6.8. K_is were calculated from Dixon plots and kinetic constants (K_t, V_{max}) for MTX uptake at pH 5.5 and 6.8 (summarized in Table 2). Consistent with the results in Figure 7, panel C, the K_is for all the substrates were dramatically decreased at pH 5.5 over those at pH 6.8. At both pHs, differences in K_is for PMX versus K_is for compounds **1** and **2** were statistically insignificant ($p > 0.05$).

To confirm GARFTase inhibition, resulting in suppressed *de novo* purine biosynthesis, suggested from our nucleoside/AICA protection experiments (Figure 6), we measured the *in vitro* inhibitory activities toward purified recombinant mouse GARFTase over a range of concentrations of the two active compounds **1** and **2** and compared the results to those for LMTX and PMX, which are established GARFTase inhibitors.[32,33] GARFTase activity was followed spectrally by monitoring the increased absorbance (at 295 nm) that accompanied one-carbon transfer from 10-formyl-5,8-dideazafolic acid to β-glycinamideribonucleotide (GAR) forming 5,8-dideazafolic acid and formyl GAR (FGAR). Compound **1** was potently inhibitory (IC_{50} of 0.06 μM) and significantly more so than compound **2**, LMTX, or PMX (Table 3).

To extend our GARFTase inhibitory results to intact cells, an *in situ* assay was used in which incorporation of [^{14}C]glycine into FGAR was measured in KB cells treated with a range of concentrations of various antifolate drugs.[17,18,32] For compounds **1** and **2**, IC_{50}s were measured that approximated their IC_{50}s for growth inhibition (Table 1) and were substantially lower than the IC_{50}s for *in situ* GARFTase inhibition by either LMTX or PMX (Table 3).

Thus, the novel pyrrolo[2,3-*d*]pyrimidine thienoyl antifolate **1** (and to a lesser extent **2**) is a remarkably potent inhibitor of proliferation in cells that express FRs or hPCFT. Despite substantial differences among inhibitions of cell proliferation by compounds **1**−**3**, this was not reflected in relative binding to FRs α and β or to hPCFT. For compounds **1** and **2**, apparent affinities for hPCFT (as reflected in

Table 3. IC_{50}s for Antifolate Analogs **1** and **2** in *in Vitro* Enzyme Assays with Recombinant Mouse GARFTase and *in Situ* GARFTase Assays with KB Cells[a]

	GARFTase assay	
antifolate	*In vitro* (μM)	*In situ* (nM)
1	0.06 (0.004)	0.63 (0.52)
2	3.31 (0.32)	7.65 (3.70)
PMX	> 20	30.0 (7.7)
LMTX	0.78(0.08)	14.0 (5.6)

[a] Results are presented as mean values from three (*in vitro*; ± standard errors in parentheses) and two (*in situ*; ± range in parentheses) experiments. For the *in situ* assays, incorporation of [^{14}C]glycine into [^{14}C]FGAR was measured in KB cells cultured in complete folate-free RPMI plus 2 nM LCV. Details are described in the Experimental Section.

K_is for inhibition of MTX transport) approached that for PMX, the most potent PCFT substrate yet reported, and binding to the transporter increased markedly at the lower pH. By contrast, due to a lack of membrane transport by hRFC, compounds **1**−**3** were all inert toward cells engineered to exclusively express hRFC but not hPCFT or FRs.

The antiproliferative effects of compounds **1** and **2** are the result of potent inhibition of GARFTase and *de novo* purine biosynthesis, measured by *in vitro* inhibition with purified GARFTase and by following incorporation of [^{14}C]glycine into FGAR *in situ* in KB cells. The ≥100-fold differences in inhibition potencies by the *in situ* assay compared with the *in vitro* GARFTase assay are likely due to synthesis of polyglutamates and increased affinities for GARFTase by polyglutamyl antifolates in intact cells analogous to LMTX.[33,34] For LMTX, the heptaglutamate form was 44-fold more potent as an inhibitor of mouse recombinant GARFTase than the monoglutamyl form.[34] The extraordinarily potent inhibition of non-polyglutamyl compound **1** toward isolated trifunctional GARFTase implies that this agent is likely to be less impacted by polyglutamylation status than other classical antifolates. Accordingly, compound **1** would be expected to significantly inhibit GARFTase in cells even in its non-polyglutamyl form and would likely be active toward antifolate-resistant tumors with decreased folypolyglutamate synthethase activity.[35]

***In Vivo* Antitumor Efficacy with Compound 1.** An *in vivo* drug efficacy trial was designed with 12 week old female ICR SCID mice implanted with subcutaneous human KB tumors. Mice were maintained *ad libitum* on folate-deficient or folate-replete diets beginning 27 days prior to tumor implantion. Serum folate concentrations were measured by *Lactobacillus casei* bioassay[36] and were 71.04 ± 12.74 nM (n = 16) for the folate-deficient mice, approximating the folate level measured in human serum.[37] For mice maintained on a folate-replete diet, serum folate was measured at 350.60 ± 33.33 nM (n = 6). Treatment and control groups were nonselectively randomized into five mice per group.

For early stage disease (see Experimental Section), mice (both folate-deficient and folate-replete) were implanted subcutaneously with human KB tumor cells, and compound **1** was administered intravenously on a Q4dx4 schedule (180 mg/kg per injection) on days 4, 8, 12, and 16 postimplantation for a total dose of 720 mg/kg. A separate treatment arm included advanced stage disease at median tumor burdens of 600−689 mg and compound **1** administration on days 29, 33, 37, and 41 days (180 mg/kg per injection). Mice were observed and weighed daily; tumors were measured twice per week.

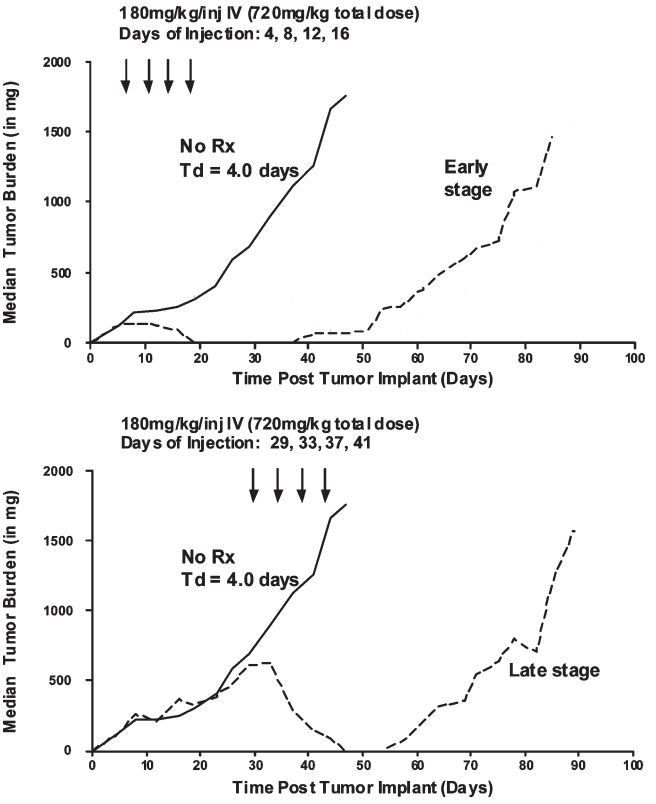

Figure 8. *In vivo* efficacy trial with compound **1**. Female ICR SCID mice (12 weeks old; 21 g average body weight) were maintained on a folate-deficient diet *ad libitum* for 27 days prior to subcutaneous tumor implantion to decrease serum folate to a concentration approximating that in human serum. Human KB tumors were implanted bilaterally, and mice were nonselectively randomized into five mice per group. Compound **1** [dissolved in 5% ethanol (v/v), 1% Tween-80 (v/v), 0.5% $NaHCO_3$] was administered on a Q4dx4 schedule intravenously (0.2 mL/injection) on days 4, 8, 12, and 16 for early stage disease or on days 29, 33, 37, and 41 for advanced stage disease beginning when the KB tumor burdens were 600−689 mg. Mice were observed and weighed daily; tumors were measured twice per week. For the experiment shown, activity was significant for both early (3.5 log kill, 1/5 cures; $T - C$ = 47 days) and late (3.7 log kill, 4/5 complete remissions; $T - C$ = 49 days) stage tumors.

Compound **1** was completely ineffectual in mice with early stage disease maintained on the standard folate-replete diet (not shown). However, for mice maintained on the folate-deficient diet significant antitumor activity was measured for both early stage (3.5 log kill, 1/5 cures; $T - C$ = 47 days) (Figure 8, upper panel) and advanced stage (3.7 log kill, 4/5 complete remissions; $T - C$ = 49 days) tumors (Figure 8, lower panel). Compound **1** was also tested at a lower dose (112.5 mg/kg per injection × 4) with advanced stage disease, resulting in a 3.8 log kill and 2/5 complete remissions (not shown). Notably, animals sustained miminal to no body weight loss during early stage drug treatment in this trial (3.7% to 0% body weight loss). Advanced stage treatment resulted in 5.4% to 13.2% weight loss nadirs (days 42−46; 1−4 days after last treatment) with full recovery by days 72−77. There were no other adverse symptoms for treated control animals held up to 145 days. Compound **1** showed significant efficacies (>3 logs of kill) against both early and advanced stage KB tumors (with complete regressions) and demonstrated good "depth of activity" at two or more dose levels, suggesting a large therapeutic index that may

Table 4. Comparison of the *in Vitro* Inhibitory Activities of Compounds **1**, **4**, and **5**[a]

	IC_{50} (nM)			
compound	GARFTase *in vitro*	GARFTase *in situ*	KB	IGROV1
1	60(4)	0.63(0.52)	0.55(0.10)	0.97(0.12)
4	150(10)	6.8(0.9)	1.9(0.7)	3.6(0.9)
5	5510(820)	13.3(5.5)	4.9(1.3)	5.9(1.9)

[a] Results are presented for mean IC_{50} values (± standard errors; in parentheses) for inhibition of KB and IGROV1 cell proliferation and for *in vitro* and *in situ* GARFTase inhibition from the present (compound **1**) and previous studies (compounds **4** and **5**).[17,18]

allow treatment at lower but still effective doses with potentially less toxicity.

Thus, results of the *in vivo* efficacy trial demonstrate potent antitumor activity for compound **1** toward subcutaneously engrafted KB tumors associated with significant transport by FRs and hPCFT and a lack of membrane transport by hRFC.

Conclusions. To summarize, this paper documents our continued efforts to identify novel antifolate agents with potential selectivity for tumors expressing high-affinity FRs or PCFT over RFC. We describe a novel series of 6-substituted pyrrolo[2,3-*d*]pyrimidine antifolates with a thienoyl ring in the side chain (compounds **1**−**3**) that differ in the lengths of the methylene bridge from four to six carbons. These analogs, like several members of our previous series of 6-substituted pyrrolo[2,3-*d*]pyrimidine and thieno[2,3-*d*]-pyrimidine antifolates, are excellent substrates for FRs but not RFC and potently inhibit *de novo* purine nucleotide biosynthesis, primarily at the level of GARFTase. The four-atom chain thienoyl analog **1** is significantly more potent than the corresponding four-carbon benzoyl analogs **4** and **5** (Figure 1)[17,18] as an inhibitor of KB and IGROV1 cell proliferation and of catalytic activity of the target enzyme GARFTase both *in vitro* and *in situ* (Table 4). These results suggest that in general the pyrrolo[2,3-*d*]pyrimidine scaffold is more conducive to GARFTase inhibition than the thieno-[2,3-*d*]pyrimidine structure (compare **4** and **5**) and that this is further enhanced by the side chain thienoyl ring in place of the benzoyl ring (compare **1** and **4**). Minor differences in FR affinities between the analogs do not manifest as increased drug activity.[17,18] However, like the pyrrolo[2,3-*d*]pyrimidine benzoyl analogs[17] (but not the thieno[2,3-*d*]pyrimidines),[18] compound **1** showed excellent activity toward hPCFT-expressing cells, to an extent approximating that for the best PCFT substrate PMX. Of course, unlike PMX, transport of compound **1** by hRFC was negligible, as noted above. Compound **1** is an excellent lead analog for further structure optimization for inhibition of GARFTase and selective transport by FR and/or hPCFT over hRFC.

The selectivity for FRs over hRFC for these agents is a paradigm for selective tumor targeting given the association of FRs with malignant cells.[9,10] Similarly, for hPCFT, expression appears to be abundant in solid tumors,[12,24] whereby tumor selectivity could result from both lack of hRFC activity and optimal transport activity at pH conditions approximating those in the interstium of solid tumors.[38] Consistent with the notion of tumor-selective drug uptake, in the *in vivo* efficacy trial with human KB tumor cells, compound **1** was highly active toward both early and advanced stage tumors with nominal toxicity.

Experimental Section

All evaporations were carried out *in vacuo* with a rotary evaporator. Analytical samples were dried in a CHEM-DRY vacuum (0.2 mmHg) drying oven over P_2O_5. Melting points were determined on a MELTEMP II melting point apparatus with FLUKE 51 K/J electronic thermometer and are uncorrected. NMR spectra for proton (^{1}H) were recorded on a Bruker WH-300 (300 MHz) spectrometer. The chemical shift values are expressed in ppm (parts per million) relative to tetramethylsilane as internal standard; s = singlet, d = doublet, t = triplet, q = quartet, m = multiplet, br = broad singlet. The relative integrals of peak areas agreed with those expected for the assigned structures. Thin-layer chromatography (TLC) was performed on PE SIL G/UV silica gel plates with fluorescent indicator, and the spots were visualized under 254 and 365 nm illumination. Proportions of solvents used for TLC are by volume. Column chromatography was performed on 230−400 mesh silica gel purchased from Fisher, Somerville, NJ. Elemental analyses were performed by Atlantic Microlab, Inc., Norcross, GA. Element compositions are within ±0.4% of the calculated values. Fractional moles of water or organic solvents frequently found in some analytical samples of antifolates were not prevented despite 24−48 h of drying *in vacuo* and were confirmed where possible by their presence in the ^{1}H NMR spectra. High-resolution mass spectrometry (HRMS) was performed on a Waters Q-TOF (API-US) by Department of Chemistry, University of Pittsburgh, Pittsburgh, PA. All solvents and chemicals were purchased from Aldrich Chemical Co. and Fisher Scientific and were used as received. Elemental analysis and TLC were used to check the purity of all targeted compounds. For compounds **1** and **3**, elemental analysis confirmed >95% purity. For compound **2**, a single spot in three different solvent systems with three different R_f values confirmed >95% purity.

General Procedure for the Synthesis of Compounds 15a−c. To **11a−c** (10 mmol) in a 250 mL flask was added oxalyl chloride (7.61 g, 60 mmol) and anhydrous CH_2Cl_2 (20 mL). The resulting solution was refluxed for 1 h and then cooled to room temperature. After the solvent was evaporated under reduced pressure, the residue of **12a−c** was dissolved in 20 mL of Et_2O. The resulting solution was added dropwise to an ice-cooled diazomethane (generated *in situ* from 15 g of diazald by using Aldrich Mini Diazald apparatus) in an ice bath over 10 min. The resulting mixture was allowed to stand for 30 min and then stirred for an additional 1 h. To this solution was added 48% HBr (20 mL). The resulting mixture was refluxed for 1.5 h. After the mixture was cooled to room temperature, the organic layer was separated, and the aqueous layer was extracted with Et_2O (200 mL × 2). The combined organic layer and Et_2O extract was washed with two portions of 10% Na_2CO_3 solution and dried over Na_2SO_4. Evaporation of the solvent afforded **14a−c** in 94% yield. To a suspension of 2,6-diaminopyrimidin-4-one (1.26 g, 10 mmol) in anhydrous DMF (25 mL) were added **14a−c** (about 9.4 mmol). The resulting mixture was stirred under N_2 at room temperature for 3 days. After evaporation of solvent under reduced pressure, MeOH (20 mL) was added followed by silica gel (5 g). The resulting plug was loaded on to a silica gel column (3.5 × 12 cm^2) and eluted with $CHCl_3$ followed by 3% MeOH in $CHCl_3$ and then 5% MeOH in $CHCl_3$ ($CHCl_3/CH_3OH$, 5:1). Fractions with R_f = 0.58 (TLC) were pooled and evaporated to afford **15a−c** as white powder.

2-Amino-6-but-3-ynyl-3,7-dihydro-pyrrolo[2,3-*d*]pyrimidin-4-one (15a). Compound **15a** was prepared using the general method described for the preparation of **15a−c** from pent-4-ynoic acid **11a** (0.98 g, 10 mmol) to give 1.4 g (74%) of **15a** as white powder. Mp 230−231 °C. ^{1}H NMR (DMSO-d_6): δ 2.41−2.45 (m, 2H), 2.64−2.67 (m, 2H), 2.77 (t, J = 2 Hz, 1H), 5.93 (s, 1H), 5.98 (s, 2H), 10.13 (s, 1H), 10.81 (s, 1H). HRMS calcd for $C_{10}H_{10}N_4O$ $(M + H)^+$, 203.0933; found, 203.0925.

2-Amino-6-pent-4-ynyl-3,7-dihydro-pyrrolo[2,3-*d*]pyrimidin-4-one (15b). Compound **15b** was prepared using the general method described for the preparation of **15a**−**c** from hex-5-ynoic acid **11b** (1.12 g, 10 mmol) to give 1.1 g (51%) of **15b** as white powder. Mp 233−234 °C. ^{1}H NMR (DMSO-d_6): δ 1.64−1.79 (m, 2H), 2.14−2.20 (m, 2H), 2.58−2.61 (t, J = 10 Hz, 2H), 2.80−2.82 (t, J = 3.2 Hz, 1H), 5.95 (s, 1H), 6.53 (s, 2H), 10.70 (s, 1H), 11.14 (s, 1H).

2-Amino-6-hex-5-ynyl-3,7-dihydro-pyrrolo[2,3-*d*]pyrimidin-4-one (15c). Compound **15c** was prepared using the general method described for the preparation of **15a**−**c** from hept-6-ynoic acid **11c** (1.26 g, 10 mmol) to give 1.43 g (62%) of **15c** as white powder. Mp 236−237 °C. ^{1}H NMR (DMSO-d_6): δ 1.40−1.47 (m, 2H), 1.52−1.67 (m, 2H), 2.13−2.17 (m, 2H), 2.46 (m, 2H), 2.75−2.77 (m, 1H), 5.87 (s, 1H), 6.16 (s, 2H), 10.31 (s, 1H), 10.90 (s, 1H).

(*S*)-2-[(5-Bromo-thiophene-2-carbonyl)-amino]-pentanedioic Acid Diethyl Ester (19). \To a 250-mL round-bottomed flask was added a mixture of 5-bromo-2-thiophene-carboxylic acid (**18**) (2.07 g, 10 mmol), *N*-methylmorpholine (1.82 g, 18 mmol), 2-chloro-4,6-dimethoxy-1,3,5-triazine (3.17 g, 18 mmol) and anhydrous DMF (20 mL). After 1.5 h, *N*-methylmorpholine (1.82 g, 18 mmol) and L-glutamic acid diethylester hydrochloride (3.6 g, 15 mmol) were added to the flask. The reaction mixture was then stirred at room temperature for 12 h. After evaporation of solvent under reduced pressure, MeOH (20 mL) was added followed by silica gel (5 g). The resulting plug was loaded onto a silica gel column (3.5 × 12 cm^2) and eluted with $CHCl_3$ followed by 1% MeOH in $CHCl_3$. Fractions with R_f = 0.45 (TLC) (Hexane/EtOAe, 2:1) were pooled and evaporated to afford **19** as colorless liquid. ^{1}H NMR (DMSO-d_6): δ 1.13−1.19 (m, 6H), 1.96−2.07 (m, 2H), 2.40−2.43 (t, J = 9 Hz, 2H), 4.00−4.12 (m, 4H), 4.35−4.40 (m, 1H), 7.30−7.31 (d, J = 5 Hz, 1H), 7.69−7.71 (d, J = 5 Hz, 1H), 8.83−8.84 (d, J = 9 Hz, 1H).

General Procedure for the Synthesis of Compounds 16a−c. To a 250-mL round-bottomed flask equipped with a magnetic stirrer and gas inlet was added a mixture of tetrakis-(triphenylphosphine)palladium(0) (185 mg, 0.16 mmol), triethylamine (1.01 g, 10 mmol), **19** (588 mg, 1.5 mmol), and anhydrous DMF (20 mL). To the stirred mixture, under N_2 were added copper(I) iodide (30 mg, 0.16 mmol) and **15a**−**c** (1 mmol), and the reaction mixture was stirred at room temperature overnight (17−18 h). After evaporation of solvent under reduced pressure, MeOH (20 mL) was added followed by silica gel (0.5 g). The resulting plug was loaded onto a silica gel column (3.5 × 12 cm^2) and eluted with $CHCl_3$ followed by 3% MeOH in $CHCl_3$ and then 5% MeOH in $CHCl_3$. Fractions with R_f = 0.53 (TLC) ($CHCl_3$/CH_3OH, 5:1) were pooled and evaporated to afford **16a**−**c** as brown powder.

(*S*)-2-({5-[4-(2-Amino-4-oxo-4,7-dihydro-3*H*-pyrrolo[2,3-*d*]-pyrimidin-6-yl)-but-1-ynyl]-thiophene-2-carbonyl}-amino)-pentanedioic Acid Diethyl Ester (16a). Compound **16a** was prepared using the general method described for the preparation of **16a**−**c** from **15a** (202 mg, 1 mmol) to give 386 mg (75%) of **16a** as brown powder. Mp 81−82 °C. ^{1}H NMR (DMSO-d_6): δ 1.16−1.21 (m, 6H), 1.93−2.15 (m, 2H), 2.40−2.45 (t, J = 10 Hz, 2H), 3.06−3.15 (m, 4H), 4.01−4.15 (m, 4H), 4.35−4.43 (m, 1H), 6.00 (s, 1H), 6.04 (s, 2H), 7.22−7.23 (d, J = 5.2 Hz, 1H), 7.77−7.78 (d, J = 5.2 Hz, 1H), 8.83−8.85 (d, J = 10 Hz, 1H), 10.18 (s, 1H), 10.89 (s, 1H). HRMS calcd for $C_{24}H_{27}N_5O_6S$ $(M + H)^+$, 514.1760; found, 514.1753.

(*S*)-2-({5-[5-(2-Amino-4-oxo-4,7-dihydro-3*H*-pyrrolo[2,3-*d*]-pyrimidin-6-yl)-pent-1-ynyl]-thiophene-2-carbonyl}-amino)-pentanedioic Acid Diethyl Ester (16b). Compound **16b** was prepared using the general method described for the preparation of **16a**−**c** from **15b** (216 mg, 1 mmol) to give 380 mg (72%) of **16b** as brown powder. Mp 84−85 °C. ^{1}H NMR (DMSO-d_6): δ 1.16−1.20 (m, 6H), 1.81−1.90 (m, 2H), 1.92−2.13 (m, 2H), 2.40−2.45 (t, J = 10 Hz, 2H), 2.46 (m, 2H), 2.59−2.64 (t, J = 9.6 Hz, 2H), 4.00−4.14 (m, 4H), 4.35−4.43 (m, 1H), 5.91 (s, 1H), 5.99 (s, 2H), 7.24−7.25 (d, J = 5.2 Hz, 1H), 7.77−7.78 (d, J = 5.2 Hz, 1H), 8.82−8.84 (d, J = 10 Hz, 1H), 10.14 (s, 1H), 10.86 (s, 1H).

(*S*)-2-({5-[6-(2-Amino-4-oxo-4,7-dihydro-3*H*-pyrrolo[2,3-*d*]-pyrimidin-6-yl)-hex-1-ynyl]-thiophene-2-carbonyl}-amino)-pentanedioic Acid Diethyl Ester (16c). Compound **16c** was prepared using the general method described for the preparation of **16a**−**c** from **15c** (230 mg, 1 mmol) to give 396 mg (73%) of **16c** as brown powder. Mp 85−86 °C. ^{1}H NMR (DMSO-d_6): δ 1.13−1.19 (m, 6H), 1.48−1.57 (m, 2H), 1.62−1.71 (m, 2H), 1.91−2.12 (m, 2H), 2.39−2.43 (t, J = 7.6 Hz, 2H), 2.46−2.48 (m, 4H), 4.00−4.12 (m, 4H), 4.34−4.40 (m, 1H), 5.87 (s, 1H), 5.96 (s, 2H), 7.23−7.24 (d, J = 3.6 Hz, 1H), 7.75−7.76 (d, J = 3.6 Hz, 1H), 8.80−8.82 (d, J = 7.6 Hz, 1H), 10.12 (s, 1H), 10.81 (s, 1H).

General Procedure for the Synthesis of Compounds 17a−c. To a Parr flask were added **16a**−**c** (0.75 mmol), 10% palladium on activated carbon (120 mg), and MeOH (100 mL). Hydrogenation was carried out at 55 psi of H_2 for 4 h. The reaction mixture was filtered through Celite, washed with MeOH (100 mL), and concentrated under reduced pressure to give **17a**−**c** as yellow powder.

(*S*)-2-({5-[4-(2-Amino-4-oxo-4,7-dihydro-3*H*-pyrrolo[2,3-*d*]-pyrimidin-6-yl)-butyl]-thiophene-2-carbonyl}-amino)-pentanedioic Acid Diethyl Ester (17a). Compound **17a** was prepared using the general method described for the preparation of **17a**−**c** from **16a** (386 mg, 0.75 mmol) to give 369 mg (95%) of **17a** as yellow powder. Mp 74−75 °C. ^{1}H NMR (DMSO-d_6): δ 1.13−1.20 (m, 6H), 1.62 (m, 4H), 1.89−2.13 (m, 2H), 2.39−2.44 (t, J = 10 Hz, 2H), 2.69 (m, 2H), 2.81 (m, 2H), 4.00−4.13 (m, 4H), 4.34−4.42 (m, 1H), 5.85 (s, 1H), 5.97 (s, 2H), 6.88−6.89 (d, J = 4.8 Hz, 1H), 7.67−7.68 (d, J = 4.8 Hz, 1H), 8.60−8.63 (d, J = 10 Hz, 1H), 10.13 (s, 1H), 10.81 (s, 1H). HRMS calcd for $C_{24}H_{31}N_5O_6S$ $(M + H)^+$, 518.2073; found, 518.2077.

(*S*)-2-({5-[5-(2-Amino-4-oxo-4,7-dihydro-3*H*-pyrrolo[2,3-*d*]-pyrimidin-6-yl)-pentyl]-thiophene-2-carbonyl}-amino)-pentanedioic Acid Diethyl Ester (17b). Compound **17b** was prepared using the general method described for the preparation of **17a**−**c** from **16b** (380 mg, 0.72 mmol) to give 360 mg (94%) of **17b** as yellow powder. Mp 77−78 °C. ^{1}H NMR (DMSO-d_6): δ 1.12−1.21 (m, 8H), 1.53−1.67 (m, 4H), 1.91−2.14 (m, 2H), 2.39−2.43 (t, J = 10 Hz, 2H), 2.46 (m, 2H), 2.77−2.82 (t, J = 9.6 Hz, 2H), 4.00−4.14 (m, 4H), 4.33−4.41 (m, 1H), 5.84 (s, 1H), 5.97 (s, 2H), 6.88−6.89 (d, J = 4.8 Hz, 1H), 7.68−7.69 (d, J = 4.8 Hz, 1H), 8.60−8.63 (d, J = 10 Hz, 1H), 10.12 (s, 1H), 10.79 (s, 1H).

(*S*)-2-({5-[6-(2-Amino-4-oxo-4,7-dihydro-3*H*-pyrrolo[2,3-*d*]-pyrimidin-6-yl)-hexyl]-thiophene-2-carbonyl}-amino)-pentanedioic Acid Diethyl Ester (17c). Compound **17c** was prepared using the general method described for the preparation of **17a**−**c** from **16c** (396 mg, 0.73 mmol) to give 379 mg (94%) of **17c** as yellow powder. Mp 78−79 °C. ^{1}H NMR (DMSO-d_6): δ 1.15−1.19 (m, 6H), 1.23−1.31 (m, 4H), 1.47−1.68 (m, 4H), 1.90−2.14 (m, 2H), 2.37−2.48 (m, 6H), 4.02−4.12 (m, 4H), 4.33−4.41 (m, 1H), 5.84 (s, 1H), 5.96 (s, 2H), 7.08−7.09 (d, J = 3.6 Hz, 1H), 7.78−7.79 (d, J = 3.6 Hz, 1H), 8.72−8.74 (d, J = 7.6 Hz, 1H), 10.11 (s, 1H), 10.79 (s, 1H).

General Procedure for the Synthesis of Target Compounds 1, 2, and 3. To a solution of **17a**−**c** (0.7 mmol) in MeOH (10 mL) was added 1 N NaOH (10 mL), and the mixture was stirred under N_2 at room temperature for 16 h. TLC showed the disappearance of the starting material (R_f = 0.45) and one major spot at the origin ($MeOH/CHCl_3$ 1:5). The reaction mixture was evaporated to dryness under reduced pressure. The residue was dissolved in water (10 mL), the resulting solution was cooled in an ice bath, and the pH was adjusted to 3−4 with dropwise addition of 1 N HCl. The resulting suspension was frozen in a dry ice−acetone bath, thawed to 4−5 °C in the refrigerator, and filtered. The residue was washed with a small amount of cold water and dried in vacuum using P_2O_5 to afford the target compounds as white powder.

(*S*)-2-({5-[4-(2-Amino-4-oxo-4,7-dihydro-3*H*-pyrrolo[2,3-*d*]-pyrimidin-6-yl)-butyl]-thiophene-2-carbonyl}-amino)-pentanedioic Acid (1). Compound **1** was prepared using the general method described for the preparation of target compounds from **17a** (369 mg, 0.71 mmol) to give 312 mg (95%) of **1** as white powder. Mp 179−180 °C. ^{1}H NMR (DMSO-d_6): δ 1.62 (m, 4H), 1.91−2.05 (m, 2H), 2.31−2.36 (t, J = 7.4 Hz, 2H), 2.69 (m, 2H), 2.81 (m, 2H), 4.29−4.43 (m, 1H), 5.87 (s, 1H), 6.10 (s, 2H), 6.87−6.88 (d, J = 4 Hz, 1H), 7.67−7.68 (d, J = 4 Hz, 1H), 8.49−8.52 (d, J = 8 Hz, 1H), 10.26 (s, 1H), 10.88 (s, 1H), 12.42 (br, 2H). HRMS calcd for $C_{20}H_{23}N_5O_6S$ (M + H)$^+$, 462.1447; found, 462.1462. Anal. ($C_{20}H_{23}N_5O_6S$), C, H, N, S, calcd for $C_{20}H_{23}N_5O_6S\cdot 0.5H_2O$: C, 51.06; H, 5.14; N, 14.88; S, 6.82. Found: C, 51.11; H, 5.07; N, 14.80; S, 6.66.

(*S*)-2-({5-[5-(2-Amino-4-oxo-4,7-dihydro-3*H*-pyrrolo[2,3-*d*]-pyrimidin-6-yl)-pentyl]-thiophene-2-carbonyl}-amino)-pentanedioic Acid (2). Compound **2** was prepared using the general method described for the preparation of target compounds from **17b** (360 mg, 0.68 mmol) to give 306 mg (95%) of **2** as white powder. Mp 181−182 °C. TLC R_f = 0.81 ($CHCl_3$/CH_3OH/NH_4OH, 3:7:2); R_f = 0.29 (EtOAc/CH_3OH/NH_4OH, 4:7:2); R_f = 0.12 (acetone/CH_3OH/NH_4OH, 5:5:1). ^{1}H NMR (DMSO-d_6): δ 1.28−1.34 (m, 2H), 1.54−1.66 (m, 4H), 1.85−2.10 (m, 2H), 2.30−2.34 (t, J = 7.4 Hz, 2H), 2.43−2.47 (t, J = 7.6 Hz, 2H), 2.76−2.80 (t, J = 7.6 Hz, 2H), 4.29−4.43 (m, 1H), 5.83 (s, 1H), 5.95 (s, 2H), 6.86−6.87 (d, J = 4 Hz, 1H), 7.66−7.67 (d, J = 4 Hz, 1H), 8.49−8.51 (d, J = 8 Hz, 1H), 10.11 (s, 1H), 10.78 (s, 1H), 12.32 (br, 2H). HRMS calcd for $C_{21}H_{25}N_5O_6S$ (M + H)$^+$, 476.1604; found, 476.1617.

(*S*)-2-({5-[6-(2-Amino-4-oxo-4,7-dihydro-3*H*-pyrrolo[2,3-*d*]-pyrimidin-6-yl)-hexyl]-thiophene-2-carbonyl}-amino)-pentanedioic Acid (3). Compound **3** was prepared using the general method described for the preparation of target compounds from **17c** (379 mg, 0.69 mmol) to give 322 mg (95%) of **3** as white powder. Mp 183−184 °C. ^{1}H NMR (DMSO-d_6): δ 1.27−1.35 (m, 2H), 1.44−1.67 (m, 6H), 1.87−2.10 (m, 2H), 2.31−2.35 (t, J = 7.4 Hz, 2H), 2.37−2.44 (m, 4H), 4.30−4.38 (m, 1H), 5.84 (s, 1H), 5.95 (s, 2H), 7.07−7.08 (d, J = 4 Hz, 1H), 7.77−7.78 (d, J = 4 Hz, 1H), 8.60−8.62 (d, J = 8 Hz, 1H), 10.12 (s, 1H), 10.79 (s, 1H), 12.46 (br, 2H). Anal. ($C_{22}H_{27}N_5O_6S$), C, H, N, S, calcd for $C_{22}H_{27}N_5O_6S\cdot 1H_2O$: C, 52.06; H, 5.75; N, 13.79; S, 6.32. Found: C, 52.39; H, 5.24; N, 13.30; S, 5.98.

Reagents for Biological Studies. [3′,5′,7-^{3}H]MTX (20 Ci/mmol), [3′,5′,7,9-^{3}H]folic acid (25 Ci/mmol), and [^{14}C(U)]-glycine (87 mCi/mmol) were purchased from Moravek Biochemicals (Brea, CA). Unlabeled folic acid was purchased from the Sigma Chemical Co. (St. Louis, MO). LCV [(6*R*,*S*)-5-formyl tetrahydrofolate] was provided by the Drug Development Branch, National Cancer Institute, Bethesda, MD. The sources of the classical antifolate drugs were as follows: MTX, Drug Development Branch, National Cancer Institute (Bethesda, MD); RTX [*N*-(5-[*N*-(3,4-dihydro-2-methyl-4-oxyquinazolin-6-ylmethyl)-*N*-methyl-amino]-2-thienoyl)-L-glutamic acid], AstraZeneca Pharmaceuticals (Maccesfield, Cheshire, England); LMTX (5,10-dideaza-5,6,7,8-tetrahydrofolate) and PMX [*N*-{4-[2-(2-amino-3,4-dihydro-4-oxo-7*H*-pyrrolo[2,3-*d*]pyrimidin-5-yl)ethyl]benzoyl}-L-glutamic acid] (Alimta), Eli Lilly and Co. (Indianapolis, IN); **7** (PT523) [N^{α}-(4-amino-4-deoxypteroyl)-N^{δ}-hemiphthaloyl-L-ornithine], Dr. Andre Rosowsky (Boston, MA); **6** (GW1843U89) [(*S*)-2-(5-(((1,2-dihydro-3-methyl-1-oxo-benzo(*f*)quinazolin-9-yl)methyl)amino)1-oxo-2-isoindolinyl)glutaric acid], GlaxoWellcome-SmithKline Co. (Research Triangle Park, NC). Both labeled and unlabeled MTX were purified by HPLC prior to use. α,β-GAR and coenzyme 10-formyl-5,8-dideazafolic acid were provided by Dr. Richard Moran (Virginia Commonwealth University, Richmond, VA). Other chemicals were obtained from commercial sources in the highest available purity.

Cell Lines and Assays of Antitumor Drug Activities. RFC- and FRα-null MTXRIIOua^{R}2−4 (R2) CHO cells were gifts from Dr. Wayne Flintoff (University of Western Ontario)[31] and were cultured in α-minimal essential medium (MEM) supplemented with 10% bovine calf serum (Invitrogen, Carlsbad, CA), penicillin−streptomycin solution and L-glutamine at 37 °C with 5% CO_2. PC43-10 cells are R2 cells transfected with hRFC.[30] RT16 cells are R2 cells transfected with human FRα, and D4 cells are R2 cells transfected with human FRβ.[17] R2/hPCFT4 cells were prepared by transfection of R2 cells with a hPCFT cDNA, epitope tagged at the C-terminus with Myc-His6 (hPCFT$^{Myc\text{-}His6}$) and cloned in pCDNA3.1.[18] All the R2 transfected cells (PC43-10, RT16, D4, R2/hPCFT4) were routinely cultured in α-MEM plus 1.5 mg/mL G418. Prior to the cytotoxicity assays (see below), RT16 and D4 cells were cultured in complete folate-free RPMI1640 (without added folate) for 3 days.

KB human cervical cancer cells were purchased from the American Type Culture Collection (Manassas, VA), whereas IGROV1 ovarian carcinoma cells were a gift of Dr. Manohar Ratnam (Medical University of Ohio). Cells were routinely cultured in folate-free RPMI1640 medium, supplemented with 10% fetal bovine serum, penicillin−streptomycin solution, and 2 mM L-glutamine at 37 °C with 5% CO_2.

For growth inhibition assays, cells (CHO, KB, or IGROV1) were plated in 96 well dishes (∼2500−5000 cells/well, total volume of 200 μL medium) with a broad range of antifolate concentrations. The medium was RPMI1640 (contains 2.3 μM folic acid) with 10% dialyzed serum and antibiotics for experiments with R2 and PC43-10 cells. For RT16, D4, KB, and IGROV1 cells, the cells were cultured in folate-free RPMI media with 10% dialyzed fetal bovine serum (Invitrogen) and antibiotics supplemented with 2 nM LCV. The requirement for FR-mediated drug uptake in these assays was established in a parallel incubation including 200 nM folic acid. For R2/hPCFT4 cells, the medium was folate-free RPMI1640 (pH 7.2) containing 25 nM LCV, supplemented with 10% dialyzed fetal bovine serum (Invitrogen) and antibiotics. Cells were routinely incubated for up to 96 h, and metabolically active cells (a measure of cell viability) were assayed with CellTiter-blue cell viability assay (Promega, Madison, WI), with fluorescence measured (590 nm emission, 560 nm excitation) using a fluorescence plate reader. Raw data were exported from Softmax Pro software to an Excel spreadsheet for analysis and determinations of IC_{50}s, corresponding to the drug concentrations that result in 50% loss of cell growth.

For some of the *in vitro* growth inhibition studies, the inhibitory effects of the antifolate inhibitors on *de novo* thymidylate biosynthesis (i.e., TS) and *de novo* purine biosynthesis (GARFTase and AICARFTase) were tested by coincubations with thymidine (10 μM) and adenosine (60 μM), respectively. For *de novo* purine biosynthesis, additional protection experiments used AICA (320 μM) as a means of distinguishing inhibitory effects at GARFTase from those at AICARFTase.[17,18,32]

For assays of colony formation in the presence of the antifolate drugs, KB cells were harvested and diluted, and 200 cells were plated into 60 mm dishes in folate-free RPMI1640 medium supplemented with 2 nM LCV, 10% dialyzed fetal bovine serum, penicillin−streptomycin, and 2 mM L-glutamine in the presence of antifolate drugs. The dishes were incubated at 37 °C with 5% CO_2 for 10−14 days. At the end of the incubations, the dishes were rinsed with Dulbecco's phosphate-buffered saline (DPBS), 5% trichloroacetic acid, and borate buffer (10 mM, pH 8.8), followed by 30 min incubation in 1% methylene blue in the borate buffer. The dishes were rinsed with the borate buffer, and colonies were counted for calculating percent colony-forming efficiency normalized to control.

FR Binding Assay. [^{3}H]Folic acid binding was used to assess levels of surface FRs.[17] Briefly, cells (e.g., RT16 or D4; ∼1.6 × 10^6) were rinsed twice with Dulbecco's phosphate-buffered saline (DPBS) followed by two washes in acidic buffer (10 mM sodium acetate, 150 mM NaCl, pH 3.5) to remove

FR-bound folates. Cells were washed twice with ice-cold HEPES-buffered saline (20 mM HEPES, 140 mM NaCl, 5 mM KCl, 2 mM $MgCl_2$, 5 mM glucose, pH 7.4; HBS), then incubated in HBS with [^{3}H]folic acid (50 nM, specific activity 0.5 Ci/mmol) in the presence and absence of a range of concentrations of unlabeled folic acid or antifolate for 15 min at 0 °C. The dishes were rinsed three times with ice-cold HBS, after which the cells were solubilized with 0.5 N sodium hydroxide and aliquots measured for radioactivity and protein contents. Protein concentrations were measured with Folin phenol reagent.[39] Bound [^{3}H]folic acid was calculated as pmol/mg protein. Relative binding affinities for assorted folate/antifolate substrates were calculated as the inverse molar ratios of unlabeled ligands required to inhibit [^{3}H]folic acid binding by 50%. By definition, the relative affinity of folic acid is 1.

Transport Assays. For transport assays, R2/hPCFT4, pC43-10, and R2(VC) CHO cells grown as monolayers were used to seed spinner flasks. For experiments to determine the inhibitions of transport by antifolate substrates, cells were collected and washed with DPBS and resuspended in 2 mL of physiologic Hank's balanced salts solution (HBSS) for PC43-10 cells and in HBS adjusted to pH 7.2 or 6.8 or 4-morpholinepropanesulfonic acid (MES)-buffered saline (20 mM MES, 140 mM NaCl, 5 mM KCl, 2 mM $MgCl_2$, and 5 mM glucose) adjusted to pH 6.5, 6.0, or 5.5 for R2/hPCFT4 cells. In either case, uptakes of [^{3}H]MTX (0.5 μM) were measured over 2 min at 37 °C in the presence and absence of unlabeled antifolates (10 μM). Uptakes of [^{3}H]MTX were quenched with ice-cold DPBS. Cells were washed with ice-cold DPBS (3×) and solubilized with 0.5 N NaOH. Levels of intracellular radioactivity were expressed as pmol/mg protein, calculated from direct measurements of radioactivity and protein contents of cell homogenates. Protein concentrations were measured with Folin phenol reagent.[39] Percent MTX transport inhibition was calculated by comparing level of [^{3}H]MTX uptake in the presence and absence of the inhibitors. Kinetic constants (K_t, V_{max}) and K_is were calculated from Lineweaver−Burke and Dixon plots, respectively. These methods are analogous to those previously published.[31]

***In Vitro* GARFTase Enzyme Inhibition Assay.** Purified recombinant mouse GARFTase enzyme was a gift from Dr. Richard Moran (Virginia Commonwealth University, Richmond, VA).[34] Inhibition of GARFTase catalytic activity was measured as previously described.[17,18] Briefly, enzyme activity was assayed spectrophotometrically at 37 °C using GARFTase (0.75 nM), α,β-GAR (11 μM), and coenzyme 10-formyl-5,8-dideazafolic acid (10 μM) in HEPES buffer (75 mM, pH 7.5) with or without antifolate inhibitor (10−30 000 nM). The absorbance of the reaction product, 5,8-dideazafolic acid, was monitored at 295 nM over the first minute as a measure of the initial rate of enzyme activity. IC_{50}s were calculated as the concentrations of inhibitors that resulted in a 50% decrease in the initial velocity of the GARFTase reaction.

***In Situ* GARFT Enzyme Inhibition Assay.** Incorporation of [^{14}C]glycine into [^{14}C]FGAR, as an *in situ* measure of endogenous GARFTase activity, was described by Beardsley et al.[32] and modified by Deng et al.[17] For these experiments, KB cells were seeded in 4 mL of complete folate-free RPMI1640 plus 2 nM LCV in 60 mm dishes at a density of 2×10^6 cells per dish. On the next day, the medium was replaced with 2 mL of fresh complete folate-free RPMI1640 plus 2 nM LCV (without supplementing glutamine). Azaserine (4 μM final concentration) was added in the presence and absence of the antifolate inhibitors (0.1, 1, 10, 100, or 1000 nM). After 30 min, L-glutamine (final concentration, 2 mM) and [^{14}C]glycine (tracer amounts; final specific activity 0.1 mCi/L) were added. Incubations were at 37 °C for 15 h, at which time cells were washed (one-time) with ice-cold folate-free RPMI1640 plus serum. Cell pellets were dissolved in 2 mL of 5% trichloroacetic acid at 0 °C. Cell debris was removed by centrifugation (the cell protein contents in the pellets were measured), and the supernatants were extracted twice with 2 mL of ice-cold ether. The aqueous layer was passed through a 1 cm column of AG1×8 (chloride form), 100−200 mesh (Bio-Rad), washed with 10 mL of 0.5 N formic acid and then 10 mL of 4 N formic acid, and finally eluted with 8 mL of 1 N HCl. The elutants were collected and determined for radioactivity. The accumulation of radioactive FGAR was calculated as pmol per mg protein over a range of inhibitor concentrations. IC_{50}s were calculated as the concentrations of inhibitors that resulted in a 50% decrease in FGAR synthesis.

***In Vivo* Efficacy Study of Compound 1.** The methods of protocol design, drug treatment, toxicity evaluation, data analysis, quantification of tumor cell kill, tumor model systems, and the biological significance of the drug treatment results with transplantable tumors have been described previously.[40−44]

Cultured KB human nasopharyngeal tumor cells grown in folate-deficient media were implanted subcutaneously (5×10^6 cells/flank) to establish a solid tumor xenograft model in female ICR SCID mice (obtained from the NIH DCT/DTP Animal Production Program, Frederick, MD). For the efficacy study, mice were 12 weeks old on day 0 (tumor implant) with an average body weight of 21 g (range 20−22 g). Mice were supplied food and water *ad libitum*. Study mice were maintained on either a folate-deficient diet from Harlan-Teklad (TD.00434) or a folate-replete diet from Lab Diet (5021; autoclavable mouse breeder diet) starting 27 days before subcutaneous tumor implant to ensure serum folate levels would approximate those of humans. Folate serum levels were determined prior to tumor implant and poststudy via *L. casei* bioassay.[36]

The animals were pooled and implanted bilaterally subcutaneously with 30−60 mg tumor fragments by a 12 gauge trocar and again pooled before unselective distribution to the various treatment and control groups. For early stage tumors, chemotherapy was begun 4 days after tumor implantation, when the number of cells was relatively small (10^7−10^8 cells; before the established limit of palpation). For advanced stage tumors, the tumors reached a median tumor burden of 689 mg (average 715 mg) for the no treatment controls and 614 mg (average 711 mg) for the compound **1**-treated group before first treatment commenced on day 29. Tumors were measured with a caliper two or three times weekly (depending on the doubling time of the tumor). Mice were sacrificed when the cumulative tumor burden reached 1500 mg. Tumor weights were estimated from two-dimensional measurements [i.e., tumor mass (in mg) = $(ab^2)/2$, where a and b are the tumor length and width in mm, respectively]. For calculation of end points, both tumors on each mouse were added together, and the total mass per mouse was used.

The following quantitative end points were used to assess antitumor activity: (i) tumor growth delay [$T - C$, where T is the median time in days required for the treatment group tumors to reach a predetermined size (e.g., 1000 mg) and C is the median time in days for the control group tumors to reach the same size; tumor-free survivors are excluded from these calculations] and (ii) calculation of tumor cell kill [$\log_{10}$ cell kill total (gross) = $(T - C)/(3.32T_d)$, where $T - C$ is the tumor growth delay as described above and T_d is the tumor volume doubling time in days, estimated from the best fit straight line from a log−linear growth plot of control group tumors in exponential growth (100−800 mg range)].

Acknowledgment. This work was supported in part by grants from the National Institutes of Health, National Cancer Institute, CA125153 (A.G.) and CA53535 (L.H.M.), and a pilot grant from the Barbara Ann Karmanos Cancer Institute. Ms. Kugel Desmoulin was supported by a Doctoral Research Award from the Canadian Institutes of Health Research (CIHR). We thank Dr. Richard Moran for providing recombinant mouse GARFTase and assays reagents.

Supporting Information Available: Elemental analysis and high-resolution mass spectra (HRMS) (ESI). This material is available free of charge via the Internet at http://pubs.acs.org.

References

(1) Monahan, B. P.; Allegra, C. J. Antifolates. In *Cancer Chemotherapy and Biotherapy*, 4th ed.; Chabner, B. A., Longo, D. L., Eds.; Lippincott-Raven: Philadelphia, 2001; pp 109−148.

(2) Hazarika, M.; White, R. M.; Johnson, J. R.; Pazdur, R. FDA Drug Approval Summaries: Pemetrexed (Alimta). *Oncologist* **2004**, *9*, 482–488.

(3) Scagliotti, G. V.; Parikh, P.; von Pawel, J.; Biesma, B.; Vansteenkiste, J.; Manegold, C.; Serwatowski, P.; Gatzemeier, U.; Digumarti, R.; Zukin, M.; Lee, J. S.; Mellemgaard, A.; Park, K.; Patil, S.; Rolski, J.; Goksel, T.; de Marinis, F.; Simms, L.; Sugarman, K. P.; Gandara, D. Phase III Study Comparing Cisplatin Plus Gemcitabine with Cisplatin Plus Pemetrexed in Chemotherapy-Naive Patients with Advanced-Stage Non-Small-Cell Lung Cancer. *J. Clin. Oncol.* **2008**, *26*, 3543–3551.

(4) Ciuleanu, T.; Brodowicz, T.; Zielinski, C; Kim, J. H.; Krzakowski, M.; Laack, E.; Wu, Y. L.; Bover, I.; Begbie, S.; Tzekova, V.; Cucevic, B.; Pereira, J. R.; Yang, S. H.; Madhavan, J.; Sugarman, K. P.; Peterson, P.; John, W. J.; Krejcy, K.; Belani, C. P. Maintenance Pemetrexed Plus Best Supportive Care versus Placebo Plus Best Supportive Care for Non-Small-Cell Lung Cancer: A Randomised, Double-Blind, Phase 3 Study. *Lancet* **2009**, *374*, 1432–1440.

(5) Chu, E.; Callender, M. A.; Farrell, M. P.; Schmitz, J. C. Thymidylate Synthase Inhibitors as Anticancer Agents: From Bench to Bedside. *Cancer Chemother. Pharmacol.* **2003**, *52* (Suppl. 1), S80–89.

(6) Matherly, L. H.; Goldman, I. D. Membrane Transport of Folates. *Vitam. Horm.* **2003**, *66*, 403–456.

(7) Matherly, L. H.; Hou, Z.; Deng, Y. Human Reduced Folate Carrier: Translation of Basic Biology to Cancer Etiology and Therapy. *Cancer Metastasis Rev.* **2007**, *26*, 111–128.

(8) Zhao, R.; Matherly, L. H.; Goldman, I. D. Membrane Transporters and Folate Homeostasis; Intestinal Absorption, Transport into Systemic Compartments and Tissues. *Expert Rev. Mol. Med.* **2009**, *11*, No. e4.

(9) Salazar, M. D.; Ratnam, M. The Folate Receptor: What Does It Promise in Tissue-Targeted Therapeutics? *Cancer Metastasis Rev.* **2007**, *26*, 141–152.

(10) Elnakat, H.; Ratnam, M. Distribution, Functionality and Gene Regulation of Folate Receptor Isoforms: Implications in Targeted Therapy. *Adv. Drug Delivery* **2004**, *56*, 1067–1084.

(11) Qiu, A.; Jansen, M.; Sakaris, A.; Min, S. H.; Chattopadhyay, S; Tsai, E.; Sandoval, C.; Zhao, R; Akabas, M. H.; Goldman, I. D. Identification of an Intestinal Folate Transporter and the Molecular Basis for Hereditary Folate Malabsorption. *Cell* **2006**, *127*, 917–928.

(12) Zhao, R.; Goldman, I. D. The Molecular Identity and Characterization of a Proton-Coupled Folate Transporter-PCFT; Biological Ramifications and Impact on the Activity of Pemetrexed. *Cancer Metastasis Rev.* **2007**, *26*, 129–139.

(13) Reddy, J. A.; Haneline, L. S.; Srour, E. F.; Antony, A. C.; Clapp, D. W.; Low, P. S. Expression and Functional Characterization of the Beta-Isoform of the Folate Receptor on CD34(+) Cells. *Blood* **1999**, *93*, 3940–3948.

(14) Leamon, C. P.; Reddy, J. A.; Vlahov, I. R.; Westrick, E.; Dawson, A.; Dorton, R.; Vetzel, M.; Santhapuram, H. K.; Wang, Y. Preclinical Antitumor Activity of a Novel Folate-Targeted Dual Drug Conjugate. *Mol. Pharmaceutics* **2007**, *4*, 659–667.

(15) Lu, Y.; Wu, J.; Gonit, M.; Yang, X.; Lee, A.; Xiang, G.; Li, H.; Liu, S.; Marcucci, G.; Ratnam, M.; Lee, R. J. Role of Formulation Composition in Folate Receptor-Targeted Liposomal Doxorubicin Delivery to Acute Myelogenous Leukemia Cells. *Mol. Pharmaceutics* **2007**, *4*, 707–712.

(16) Muller, C.; Forrer, F.; Schibli, R.; Krenning, E. P.; de Jong, M. SPECT Study of Folate Receptor-Positive Malignant and Normal Tissues in Mice Using a Novel 99mTc-Radiofolate. *J. Nucl. Med.* **2008**, *49*, 310–317.

(17) Deng, Y.; Wang, Y.; Cherian, C.; Hou, Z.; Buck, S. A.; Matherly, L. H.; Gangjee, A. Synthesis and Discovery of High Affinity Folate Receptor-Specific Glycinamide Ribonucleotide Formyltransferase Inhibitors with Antitumor Activity. *J. Med. Chem.* **2008**, *51*, 5052–5063.

(18) Deng, Y.; Zhou, X.; Kugel Desmoulin, S.; Wu, J.; Cherian, C.; Hou, Z.; Matherly, L. H.; Gangjee, A. Synthesis and Biological Activity of a Novel Series of 6-Substituted Thieno[2,3-*d*]pyrimidine Antifolate Inhibitors of Purine Biosynthesis with Selectivity for High Affinity Folate Receptors over the Reduced Folate Carrier and Proton-Coupled Folate Transporter for Cellular Entry. *J. Med. Chem.* **2009**, *52*, 2940–2951.

(19) Jansen, G. Receptor- and Carrier-Mediated Transport Systems for Folates and Antifolates: Exploitation for Folate Chemotherapy and Immunotherapy. In *Anticancer Development Guide: Antifolate Drugs in Cancer Therapy*; Jackman, A. L., Ed.; Humana Press Inc.: Totowa, NJ, 1999; pp 293−321.

(20) Jones, T. R.; Calvert, A. H.; Jackman, A. L.; Eakin, M. A.; Smithers, M. J.; Betteridge, R. F.; Newell, D. R.; Hayter, A. J.; Stocker, A.; Harland, S. J.; et al. Quinazoline Antifolates Inhibiting Thymidylate Synthase: Variation of the N10 Substituent. *J. Med. Chem.* **1985**, *28*, 1468–1476.

(21) Jones, T. R.; Calvert, A. H.; Jackman, A. L.; Brown, S. J.; Jones, M.; Harrap, K. R. A Potent Antitumour Quinazoline Inhibitor of Thymidylate Synthetase: Synthesis, Biological Properties and Therapeutic Results in Mice. *Eur. J. Cancer* **1981**, *17*, 11–19.

(22) Theti, D. S.; Bavetsias, V.; Skelton, L. A.; Titley, J.; Gibbs, D.; Jansen, G.; Jackman, A. L. Selective Delivery of CB300638, A Cyclopenta[g]quinazoline-based Thymidylate Synthase Inhibitor into Human Tumor Cell Lines Overexpressing the Alpha-Isoform of the Folate Receptor. *Cancer Res.* **2003**, *63*, 3612–3618.

(23) Gibbs, D. D.; Theti, D. S.; Wood, N.; Green, M.; Raynaud, F.; Valenti, M.; Forster, M. D.; Mitchell, F.; Bavetsias, V.; Henderson, E.; Jackman, A. L. BGC 945, A Novel Tumor-Selective Thymidylate Synthase Inhibitor Targeted to Alpha-Folate Receptor-Overexpressing Tumors. *Cancer Res.* **2005**, *65*, 11721–11728.

(24) Kugel Desmoulin, S.; Wang, Y.; Wu, J.; Hou, Z.; Cherian, C.; Gangjee, A.; Matherly, L. H. Discovery of a Glycinamide Ribonucleotide Formyltransferase Inhibitor with Solid Tumor Selectivity via Its Transport by the Proton-Coupled Folate Transporter. *Abstr., Am. Assoc. Cancer Res.* **2009**, *50*, 404.

(25) Wang, L.; Kugel Desmoulin, S.; Deng, Y.; Polin, L.; Cherian, C.; Matherly, L. H.; Gangjee, A. The Design, Synthesis and *in Vitro* and *in Vivo* Evaluation of Selective FR α and *β* and PCFT Substrates with Potent GARFTase Inhibitory Activity as Antitumor Agents. *Abstr., Am. Assoc. Cancer Res.* **2009**, *50*, 463.

(26) Ray, M. S.; Muggia, F. M.; Leichman, G.; Grunberg, S. M.; Nelson, R. L.; Dyke, R. W.; Moran, R. G. Phase I Study of (6R)-5,10-Dideazatetrahydrofolate: A Folate Antimetabolite Inhibitory to De Novo Purine Synthesis. *J. Natl. Cancer Inst.* **1993**, *85*, 1154–1159. Cole, J. T.; Gralla, R. J.; Kardinal, C. G.; Rivera, N. P. Lometrexol (DDATHF): Phase I Trial of a Weekly Schedule of This New Antifolate. *Proc. Am. Assoc. Cancer Res.* **1992**, *33*, 2468. Wedge, S. R.; Laohavinij, S.; Taylor, G. A.; Newell, D. R.; Charlton, C. J.; Proctor, M.; Chapman, R.; Simmons, D.; Oakey, A.; Gumbrell, L.; Calvert, A. H. *Proc. Am. Assoc. Cancer Res.* **1993**, *34*, 1629.

(27) Budman, D. R.; Johnson, R.; Barile, B.; Bowsher, R. R.; Vinciguerra, V.; Allen, S. L.; Kolitz, J.; Ernest, C. S., II; Kreis, W.; Zervos, P.; Walling, J. Phase I and Pharmacokinetic Study of LY309887: A Specific Inhibitor of Purine Biosynthesis. *Cancer Chemother. Pharmacol.* **2001**, *47*, 525–531.

(28) Boritzki, T. J.; Zhang, C.; Bartlett, C. A.; Jackson, R. C. AG2034 A GARFT Inhibitor With Selective Cytotoxicity to Cells that Lack a G1 Checkpoint. In *Anticancer Drug Development Guide: Antifolate Drugs in Cancer Therapy*; Jackman, A. L., Ed.; Humana Press Inc.: Totowa, NJ, 1999; pp 281−292.

(29) McLeod, H. L.; Cassidy, J.; Powrie, R. H.; Priest, D. G.; Zorbas, M. A.; Synold, T. W.; Shibata, S.; Spicer, D.; Bissett, D.; Pithavala, Y. K.; Collier, M. A.; Paradiso, L. J.; Roberts, J. D. Pharmacokinetic and Pharmacodynamic Evaluation of the Clycinamide Ribonucleotide Formyltransferase Inhibitor AG2034. *Clin. Cancer. Res.* **2000**, *6*, 2677–2684.

(30) Wong, S. C.; Proefke, S. A.; Bhushan, A.; Matherly, L. H. Isolation of Human cDNAs that Restore Methotrexate Sensitivity and Reduced Folate Carrier Activity in Methotrexate Transport-Defective Chinese Hamster Ovary Cells. *J. Biol. Chem.* **1995**, *270*, 17468–17475.

(31) Flintoff, W. F.; Davidson, S. V.; Siminovitch, L. Isolation and Partial Characterization of Three Methotrexate-Resistant Phenotypes from Chinese Hamster Ovary Cells. *Som. Cell Genet.* **1976**, *2*, 245–261.

(32) Beardsley, G. P.; Moroson, B. A.; Taylor, E. C.; Moran, R. G. A New Folate Antimetabolite, 5,10-Dideaza-5,6,7,8-tetrahydrofolate is a Potent Inhibitor of de novo purine Synthesis. *J. Biol. Chem.* **1989**, *264*, 328–333.

(33) Shih, C.; Thornton, D. E. Preclinical Pharmacology Studies on the Clinical Development of a Novel Multitargeted Antifolate, MTA (LY231514). In *Anticancer Development Guide: Antifolate Drugs in Cancer Therapy*; Jackman, A. L., Ed.; Humana Press Inc.: Totowa, NJ, 1999; pp 183−201.

(34) Sanghani, S. P.; Moran, R. G. Tight Binding of Folate Substrates and Inhibitors to Recombinant Mouse Glycinamide Ribonucleotide Formyltransferase. *Biochemistry* **1997**, *36*, 10506–10516.
(35) Zhao, R.; Goldman, I. D. Resistance to Antifolates. *Oncogene* **2003**, *22*, 7431–7457.
(36) Varela-Moreiras, G.; Selhub, J. Long Term Folate Deficiency Alters Folate Content and Distribution Differently in Rat Tissues. *J. Nutr.* **1992**, *122*, 986–991.
(37) Ganji, V.; Kafai, M. R. Demographic, Lifestyle, and Health Characteristics and Serum B Vitamin Status Are Determinants of Plasma Total Homocysteine Concentration in the Post-Folic Acid Fortification Period, 1999−2004. *J. Nutr.* **2009**, *139*, 345–52.
(38) Raghunand, N.; Altbach, M. I.; van Sluis, R.; Baggett, B.; Taylor, C. W.; Bhujwalla, Z. M.; Gillies, R. J. Plasmalemmal pH-Gradients in Drug-Sensitive and Drug-Resistant MCF-7 Human Breast Carcinoma Xenografts Measured by 31P Magnetic Resonance Spectroscopy. *Biochem. Pharmacol.* **1999**, *57*, 309–312.
(39) Lowry, O. H.; Rosebrough, N. J.; Farr, A. L.; Randall, R. J. Protein Measurement with the Folin Phenol Reagent. *J. Biol. Chem.* **1951**, *193*, 265–275.
(40) Corbett, T.; Valeriote, F.; LoRusso, P.; Polin, L.; Panchapor, C.; Pugh, S.; White, K.; Knight, J.; Demchik, L.; Jones, J.; Jones, L.; Lowichik, N.; Biernat, L.; Foster, B.; Wozniak, A.; Lisow, L.; Valdivieso, M.; Baker, L.; Leopold, W.; Sebolt, J.; Bissery, M.-C.; Mattes, K.; Dzubow, J.; Rake, J.; Perni, R.; Wentland, M.; Coughlin, S.; Shaw, J. M.; Liverside, G.; Liversidge, E.; Bruno, J.; Sarpotdar, P.; Moore, R.; Patterson, G. Tumor Models and the Discovery and Secondary Evaluation of Solid Tumor Active Agents. *Int. J. Pharmacogn.* **1995**, *33* (Suppl.), 102–122.
(41) Corbett, T. H.; Valeriote, F. A.; Demchik, L.; Lowichik, N.; Polin, L.; Panchapor, C.; Pugh, S.; White, K.; Kushner, J.; Rake, J.; Wentland, M.; Golakoti, T.; Hetzel, C.; Ogino, J.; Patterson, G.; Moore, R. Discovery of Cryptophycin-1 and BCN-183577: Examples of Strategies and Problems in the Detection of Antitumor Activity in Mice. *Invest. New Drugs* **1997**, *15*, 207–218.
(42) Corbett, T. H.; Polin, L.; Roberts, B. J.; Lawson, A. J.; Leopold, W. R., III; White, K.; Kushner, J.; Paluch, J.; Hazeldine, S.; Moore, R.; Rake, J.; Horwitz, J. P. Transplantable Syngeneic Rodent Tumors: Solid Tumors of Mice. In *Tumor Models in Cancer Research*; Teicher, B., Ed.; Humana Press Inc.: Totowa, NJ, 2002l Chapter 3, pp 41−71.
(43) Corbett, T.; Polin, L.; LoRusso, P.; Valeriote, F.; Panchapor, C.; Pugh, S.; White, K. P.; Knight, J.; Demchik, L.; Jones, J.; Jones, L.; Lisow, L. *In Vivo* Methods for Screening and Preclinical Testing; Use of Rodent Solid Tumors for Drug Discovery. In *Anticancer Drug Development Guide*, 2nd ed.; Teicher, B. A., Andrews, P. A., Eds.; Humana Press Inc.: Totowa, NJ, 2004; Chapter 6, pp 99−124.
(44) Polin, L.; Valeriote, F.; White, K.; Panchapor, C.; Pugh, S.; Knight, J.; LoRusso, P.; Hussain, M; Liversidge, E.; Shaw, M.; Golakoti, T.; Patterson, G.; Moore, R.; Corbett, T. H. Treatment of Human Prostate Tumors PC-3 and TSU-PR1 with Standard and Investigational Agents in SCID Mice. *Invest. New Drugs* **1997**, *15*, 99–108.